Size-controlled highly luminescent silicon nanocrystals: A SiO/SiO_2 superlattice approach

M. Zacharias,[a] J. Heitmann, R. Scholz, and U. Kahler
Institute of Microstructure Physics, Weinberg 2, 06120 Halle, Germany

M. Schmidt and J. Bläsing
Institute of Experimental Physics, Otto-von-Guericke University, PF 4120, 39016 Magdeburg, Germany

(Received 4 April 2001; accepted for publication 5 November 2001)

Phase separation and thermal crystallization of SiO/SiO_2 superlattices results in ordered arranged silicon nanocrystals. The preparation method which is fully compatible with Si technologies enables independent control of particle size as well as of particle density and spatial position by using a constant stoichiometry of the layers. Transmission electron microscopy investigations confirm the size control in samples with an upper limit of the nanocrystal sizes of 3.8, 2.5, and 2.0 nm without decreasing the silicon nanocrystal density for smaller sizes. The nanocrystals show a strong luminescence intensity in the visible and near-infrared region. A size-dependent blueshift of the luminescence and a luminescence intensity comparable to porous Si are observed. Nearly size independent luminescence intensity without bleaching effects gives an indirect proof of the accomplishment of the independent control of crystal size and number. © *2002 American Institute of Physics.* [DOI: 10.1063/1.1433906]

Nanoscaled structures play a major role in optoelectronic and semiconductor research with many applications already in a commercial state. After intense research focused on porous silicon there remains only limited hope for active light emitting silicon-based devices. Highly porous materials are very fragile and will hardly survive standard Si technology. In addition, the surfaces of the remaining Si wires and dots are highly reactive. In the past, the influence of surface passivation like oxidation or hydrogenation on the optical properties was investigated.[1] Present Si nanocrystals research is focused on the preparation of Si nanocrystals embedded in an oxide host. Methods applied for preparation are Si ion implantation into high quality oxides,[2] sputtering of Si rich oxides,[3] or reactive evaporation of Si rich oxides.[4] With regard to a strong photoluminescence (PL) of the nanocrystalline Si (nc-Si) in the visible spectral range the control of size, passivation, and density is mandatory. A blueshift of the luminescence is observed with decreasing nanocrystal size. The size control is realized in all these methods by changing the chemical stoichiometry of the films. Reduction of the implanted Si dose or the O enrichment are the usual ways for a decrease in nanocrystal size. However, by decreasing the nanocrystal size into the desired range the density of the nanocrystals is reduced simultaneously. In addition, there is only a limited control of the size distribution. High temperature annealing results in diffusion of the Si atoms and in Si clusters in the oxide. Crystallization occurs for cluster sizes larger than the critical crystallization radius and by using annealing temperatures above the crystallization temperature.[5] For device application accurate engineering of spatial position, size, and density of the Si nanocrystals is essential. As a first approach, the preparation of amorphous Si/SiO_2 superlattices was suggested.[6] After high temperature annealing of amorphous Si/SiO_2 superlattice the size of the formed nanocrystals is limited at least in one direction due to the Si layer thickness used.[7,8] A severe drawback of this method is that most of the nanocrystals touch each other and the layers are more like a polycrystalline film as was shown by transmission electron microscopy (TEM) investigations. This clearly limits the luminescence efficiency in the visible range due to nonradiative processes at the grain boundaries.

In this letter, we present a method for the preparation of Si nanocrystals which enables to control not only the size but also the density and the arrangements of the nanocrystals as well and independent of the stoichiometry. Strong photoluminescence (PL) and a size dependent shift of the PL position are shown as a proof for size control and passivation.

Amorphous SiO_x/SiO_2 superlattices were prepared by reactive evaporation of SiO powders in oxygen atmosphere. The films were deposited on 4 in. wafers in a conventional evaporation system with two symmetrically arranged evaporators. Rotation of the substrate enables a high homogeneity over the whole wafer. Before evaporation the chamber was pumped down to 1×10^{-7} mbar. The substrate temperature was 100 °C. In this work, a constant stoichiometry of $x\approx1$ was used for the ultrathin SiO_x layers. We prepared SiO layers with thicknesses from 3 nm (sample A) to 1 nm (sample B) and with 46–92 periods separated by SiO_2 layers of 3 and 2 nm to force the nanocrystals into a dense and layered arrangement. After deposition the samples were annealed at 1100 °C for 1 h under N_2 atmosphere.

Selected SiO/SiO_2 films were investigated by cross section TEM in CM20T and JEM-4010 electron microscopes. The cross section samples were prepared in the usual way including final Ar ion milling. Imaging the superlattice structures as deposited and after annealing was realized applying the Fresnel defocus method at medium magnifications. The formation of the nanocrystals during annealing and their

[a]Electronic mail: zacharias@mpl-halle.de

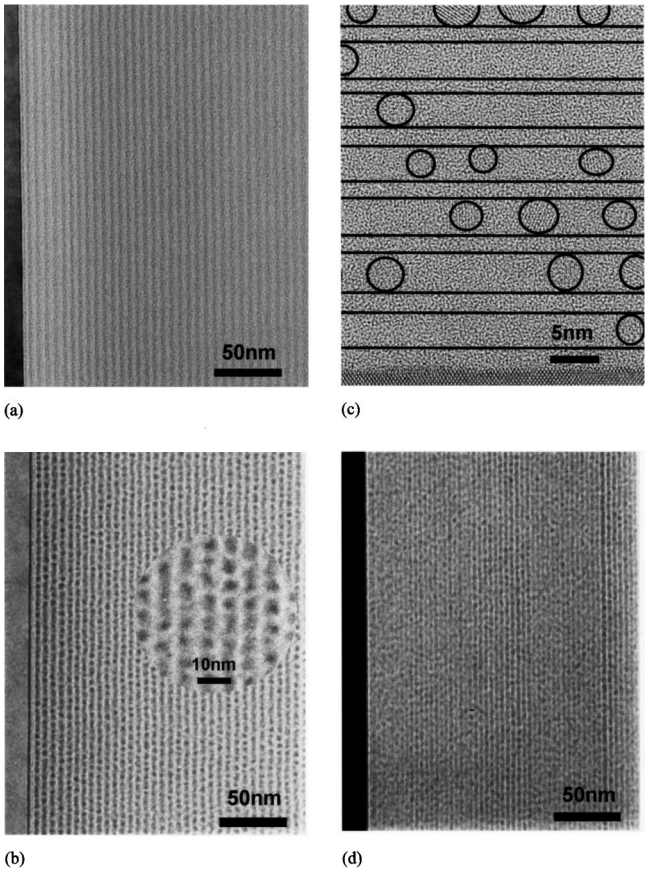

FIG. 1. Cross-sectional TEM images of SiO/SiO_2 superlattices: (a) As-prepared SiO/SiO_2 superlattice. The darker layers represent the SiO sublayers. (b) The same film after annealing. The separation of the nanocrystals by a thin oxide shell is clearly visible. (c) High resolution TEM image of the film. For clarity, the visible nanocrystals are highlighted by circles. The crystals are only found in the former SiO layers, which is emphasized by the lines in the image. (d) TEM image of a film with even thinner SiO layers ~2 nm after anneling.

sizes were confirmed in dark field images and partly under high resolution imaging conditions. The PL spectra are taken using a liquid nitrogen cooled CCD array camera attached to a single monochromator. The 325 nm line of a HeCd laser with a power of 35 mW was used as excitation source. All spectra are corrected for spectral response of the measurement system.

Figure 1(a) shows the as-prepared film of sample A with SiO and SiO_2 layers of 2.8–3.2 nm thickness. Figure 1(b) represents the same film after annealing. Clearly visible are the superlattice structure and the phase separation. The circular inset is an image zoom to demonstrate the size of the nanocrystals and their oxide separation. In high resolution [Fig. 1(c)], nanocrystals can be seen by lattice images. The arrangement in layers parallel to the substrate surface is clearly visible. Please note, that only crystals having the right orientation with respect to the incident electron beam can be seen by their lattice images. Figure 1(d) presents sample B with the SiO/SiO_2 superlattice structure but with even thinner nanocrystalline layers and therefore smaller crystals.

Using dark field conditions the upper limit of the nanocrystal sizes was estimated. The roughness of the interfaces was below 0.5 nm at both sides in the as-prepared films resulting in a size distribution of (3.3 ± 0.5) nm after annealing for sample A. The upper limit of the nanocrystal size

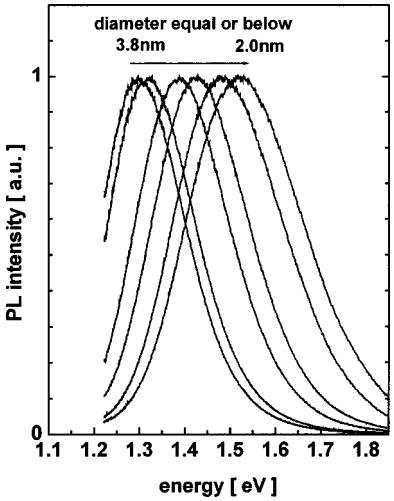

FIG. 2. Nomalized photoluminescence spectra showing a blue shift correlated with the crystal size.

estimated from dark field images are $\leqslant 3.8$ nm for sample A, and $\leqslant 2.0$ nm for sample B. No larger crystals were observed. By x-ray diffraction we estimated the average nanocrystal size using the Scherrer equation. The average size estimated from sample A was 3.4 nm (± 0.5 nm), in good agreement with the abovementioned TEM results.

Figure 2 shows the normalized luminescence spectra of the investigated films. A strong blueshift from 960 to 810 nm with decreasing nanocrystals size was observed. The PL does not show any time dependent degradation or bleaching as known for porous silicon. The PL intensity varied by around 12% compared to the PL intensity of the strongest sample but does not systematically degrade with decreasing size.

Reactive evaporation of SiO powder in oxygen atmosphere was used previously for preparation of bulk amorphous SiO_x films with x in the range between 1 and 2.[4] The high temperature annealing of such initially amorphous SiO_x films results in phase separation described by

$$SiO_x \rightarrow \frac{x}{2} SiO_2 + \left(1 - \frac{x}{2}\right) Si,$$

and in Si clusters in a SiO_2 matrix. The phase separation of the SiO_x automatically ensures that nucleated Si nanocrystals/nanoclusters are separated from each other by a SiO_2 shell. Based on the above equation the thickness of the oxide between the Si nanoclusters depends on the stoichiometry of the SiO_x as well. The crystallization of bulk SiO_x films results in randomly distributed nanocrystals with an average size depending on the original stoichiometry and a log normal size distribution. Also, an increase of the stoichiometry parameter x to 1.63 is necessary in case of thick SiO_x films for an average size of 3 nm corresponding to a drastically reduced density of nanocrystals correlated with a strong decrease in PL intensity.[4] In contrast, we used a constant stoichiometry of x around 1.0 for preparation of the thin SiO layers. The nanocrystal sizes are controlled independently by using a layer thickness equal or slightly below the desired crystal sizes. As can be seen by comparing Figs. 1(b) and 1(d) the density of the nanocrystals is even higher for the film with the ~2 nm crystals which is due to the thinner

buffer oxide layers of only 2 nm in this case. After phase separation and crystallization the nanocrystals show a size in the range of the layer thickness with small fluctuation due to the fact that by accident there might be one or even two atomic layers more on each side of the interface in agreement with the original interface roughness. Even more important is the fact that we can clearly limit the upper size of the nanocrystals with our method as can be seen by our TEM and high resolution TEM. Such control cannot be realized by either ion implantation or bulk thick SiO_x films which show inclusions of larger sizes randomly arranged in the matrix. The amorphous Si/SiO_2 films are polycrystalline after the annealing process with grain boundaries and the formation of briquettes for thicker layers.

Some of the nanocrystals visible in Fig. 1(c) seem to be smaller than the layer thickness which is due to the fact that either the TEM preparation cuts the nanocrystals at different cross positions or some of the nanocrystals are really smaller or both. Note, that the position of the nanocrystals can be controlled in growth direction due to the position of the layer. Within the layers there seems to be a self arrangement [see zoom in Fig. 1(b)] correlated to used stoichiometry and thickness of the buffer oxide in a way that for adjacent layers the nanocrystals are formed in the middle of two adjacent nanocrystals. Such an arrangement could be understood by the periodic correlated strain fluctuations of the nanocrystal network which could prefer this position for a nucleus. The self-arrangement effect is destroyed if the buffer SiO_2 layer is too thin (below 2 nm) due to the influence of the interface roughness or if the layer is to thick due to strain relaxation. The lower limit in size is given by the crystallization theory adapted to nanometer-thick layers.[5] We expect a critical crystallization diameter of around 1.8 nm for oxide interfaces and the above superlattice structure. Hence, a layer thickness of 1 nm (sample B) will most likely not result in nanocrystals of a diameter of 1 nm. As seen in Fig. 1(d) the size is slightly larger than the original layer thickness and in the range of the critical crystallization diameter. Especially for such samples the full width at half maximum (FWHM) of the size distribution is below ± 0.5 nm. Smaller crystals are not expected to be stable using equilibrium annealing conditions but could possibly be generated by using rapid thermal annealing.

The quantum confinement model predicts a blueshift of the PL peak maximum and a higher recombination probability for electron-hole pairs with decreasing crystal size. Furthermore, the absorption cross section decreases for smaller crystals and is both detection and excitation energy dependent.[9] Increasing recombination probability for decreasing crystal size could not be seen by PL intensity enhancement so far in decomposed thick SiO_x films or in implanted samples, because in such samples crystals size and number are coupled by the sample stoichiometry and thus the PL intensity for samples containing smaller crystals decreases strongly. Kahler *et al.*[4] suggested quantum confinement as the origin of the strong PL of crystallized SiO_x film and showed phonon replica in the resonant excited PL signal. The strong decrease of the PL intensity for smaller sizes by one order of magnitude observed by Kahler *et al.*[4] is in agreement with the decrease of the crystal density and the smaller absorption cross section.[9]

The observed blueshift of the PL signal with decreasing crystals size in Fig. 2 can be explained by quantum confinement taking the complete oxygen passivation of our nanocrystals into account.[10] In this case, the blueshift is smaller than expected for a recombination via free exciton states which normally is found for hydrogen passivated Si cluster. However, there is still a deviation for our smallest sizes ($d \leqslant 2$ nm) which requires further investigations. The nearly size-independent PL intensity observed in our SiO/SiO_2 superlattices indicates the accomplishment of an independent control of crystal size and number. So far we did not observe the expected increasing PL intensity for samples with decreasing crystal size. However, several additional size dependent effects such as the absorption cross section or the crystallization process itself may also play a role and influence the PL intensity.

In conclusion, the preparation of SiO_x/SiO_2 superlattices represents a simple and efficient method for fabricating highly luminescent Si nanocrystals which allows independent control of size, size distribution, and density. We can arrange the Si nanocrystals in a specific depth and for a specific number of layers and with a specific density. The thickness of the SiO layer controls the size of the crystals. The stoichiometry parameter x enables the control of the crystal density within the layers as well as the separation of the nanocrystals by a sufficient oxide barrier. In addition, the thickness of the SiO_2 layers which are used for separation of the active nanocrystalline layers controls the overall density of the nanocrystals in the films. Such control is not possible with the known preparation methods available in the literature. The process is fully compatible with normal Si technology. Also, reactive evaporation is quite simple and easy to control. In addition, other methods like electron beam evaporation, CVD, reactive rf sputtering or even pulsed laser deposition can be applied for the preparation of amorphous SiO_x/SiO_2 superlattices, and should result in a similar nanocrystalline structure after annealing. Strong photoluminescence of the samples, comparable to that of porous silicon, was observed associated with a blueshift with decreasing size of the nanocrystals. The nearly size independent PL intensity is an indirect proof of the accomplishment of the independent control of crystal size and number.

[1] L. Tsybeskov and P. M. Fauchet, Appl. Phys. Lett. **64**, 1983 (1994).
[2] T. Shimizu-Iwayama, N. Kurumado, D. E. Hole, and P. D. Townsend, J. Appl. Phys. **83**, 6018 (1998).
[3] S. Hayashi and K. Yamamoto, J. Lumin. **70**, 352 (1996).
[4] U. Kahler and H. Hofmeister, Opt. Mater. **17**, 83 (2001).
[5] M. Zacharias and P. Streitenberger, Phys. Rev. **62**, 8391 (2000).
[6] Z. H. Lu, D. J. Lockwood, and J.-M. Baribeau, Nature (London) **378**, 258 (1995).
[7] L. Tsybeskov, K. D. Hirschman, S. P. Duttagupta, M. Zacharias, and P. M. Fauchet, Appl. Phys. Lett. **72**, 43 (1998).
[8] M. Zacharias, L. Tsybeskov, K. D. Hirschman, P. M. Fauchet, J. Bläsing, P. Kohler, and P. Veit, J. Non-Cryst. Solids **227-230**, 1132 (1998).
[9] D. Kovalev, H. Heckler, G. Polisski, and F. Koch, Phys. Status Solidi B **215**, 871 (1999).
[10] M. V. Wolkin, J. Jorne, P. M. Fauchet, A. Allan, and C. Delerue, Phys. Rev. Lett. **82**, 197 (1999).